INTERNATIONAL
ENDODONTIC JOURNAL

doi:10.1111/iej.12181

Effect of bismuth oxide on white mineral trioxide aggregate: chemical characterization and physical properties

R. Grazziotin-Soares[1], M. H. Nekoofar[2,3], T. E. Davies[4], A. Bafail[3], E. Alhaddar[3], R. Hübler[5], A. L. S. Busato[1] & P. M. H. Dummer[3]

[1]School of Dentistry, Universidade Luterana do Brasil, Canoas, RS, Brazil; [2]Department of Endodontics, School of Dentistry, Tehran University of Medical Sciences, Tehran, Iran; [3]Endodontology Research Group, School of Dentistry, Cardiff University, Cardiff; [4]School of Chemistry, Cardiff University, Cardiff, UK; and [5]Materials and Nanosciences Laboratory, School of Physics, Pontifícia Universidade Católica do Rio Grande do Sul, Porto Alegre, RS, Brazil

Abstract

Grazziotin-Soares R, Nekoofar MH, Davies TE, Bafail A, Alhaddar E, Hübler R, Busato ALS, Dummer PMH. Effect of bismuth oxide on white mineral trioxide aggregate: chemical characterization and physical properties. *International Endodontic Journal*, **47**, 520–533, 2014.

Aim To assess the effect of bismuth oxide (Bi_2O_3) on the chemical characterization and physical properties of White mineral trioxide aggregate (MTA) Angelus.

Methodology Commercially available White MTA Angelus and White MTA Angelus without Bi_2O_3 provided by the manufacturer especially for this study were subjected to the following tests: Rietveld X-ray diffraction analysis (XRD), energy-dispersive X-ray analysis (EDX), scanning electron microscopy (SEM), compressive strength, Vickers microhardness test and setting time. Chemical analysis data were reported descriptively, and physical properties were expressed as means and standard deviations. Data were analysed using Student's *t*-test and Mann–Whitney U test ($P = 0.05$).

Results Calcium silicate peaks were reduced in the diffractograms of both hydrated materials. Bismuth particles were found on the surface of White MTA Angelus, and a greater amount of particles characterized as calcium hydroxide was observed by visual examination on White MTA without Bi_2O_3. The material without Bi_2O_3 had the shortest final setting time (38.33 min, $P = 0.002$), the highest Vickers microhardness mean value (72.35 MPa, $P = 0.000$) and similar compressive strength results ($P = 0.329$) when compared with the commercially available White MTA Angelus containing Bi_2O_3.

Conclusion The lack of Bi_2O_3 was associated with an increase in Vickers microhardness, a reduction in final setting time, absence of Bi_2O_3 peaks in diffractograms, as well as a large amount of calcium and a morphology characteristic of calcium hydroxide in EDX/SEM analysis.

Keywords: chemical properties, energy-dispersive X-ray, mineral trioxide aggregate, physical properties, radiopacifiers, X-ray diffraction analysis.

Received 25 February 2013; accepted 31 July 2013

Introduction

Following the introduction of mineral trioxide aggregate (MTA) for the repair of root perforations (Lee *et al.* 1993) and as a root-end filling material in endodontic surgery (Torabinejad *et al.* 1993), a large body of scientific evidence from both clinical studies (Chong *et al.* 2003, Lindeboom *et al.* 2005, Nair *et al.* 2008, Mente *et al.* 2010, Zarrabi *et al.* 2010, Erdem *et al.* 2011, von Arx *et al.* 2012) and laboratory assays (Bernabé *et al.* 2010, Zeferino *et al.* 2010, Parirokh *et al.* 2011, da Silva *et al.* 2011, Shokouhinejad *et al.* 2012) has confirmed the role of MTA as the material of choice for a range of procedures in endodontics.

Correspondence: Renata Grazziotin-Soares, Pós-Graduação em Odontologia, Universidade Luterana do Brasil (ULBRA), Av. Farroupilha, 8001, Prédio 59, 3° Andar, Bairro São José, Canoas, RS 92425-900, Brazil (Tel.: +55 51 3462 9512; Fax: +55 51 3462 9510; e-mail: regrazziotin@gmail.com).

The main crystalline phases of MTA are tricalcium silicate (Ca_3SiO_5), dicalcium silicate (Ca_2SiO_4) and tricalcium aluminate ($Ca_3Al_2O_6$), that is, the same phases as Portland cement (Camilleri *et al.* 2005a). However, MTA has to be radiopaque (Torabinejad *et al.* 1995) so as to enable its differentiation from adjacent structures on radiographs. Radiopacity was achieved for ProRoot MTA (Dentsply Maillefer, Ballaigues, Switzerland) by the addition of bismuth oxide (Bi_2O_3) to MTA powder (Portland cement) at a 4 : 1 ratio (Torabinejad & White 1995). Lower levels of radiopacifier (10.5%) are added to MTA Angelus powder (Angelus Dental Industry Products S/A, Londrina, PR, Brazil) (Camilleri *et al.* 2012), and reports have suggested that it is less radiopaque than ProRoot MTA (Camilleri & Gandolfi 2010).

The gradual addition of Bi_2O_3 as a radiopacifier to Portland cement has the potential to decrease its mechanical strength and increase its porosity, as a result of the larger amount of unreacted water that remains (Coomaraswamy *et al.* 2007). However, other studies have failed to observe undesirable effects associated with the addition of Bi_2O_3 to Portland cement in terms of biocompatibility (Coutinho-Filho *et al.* 2008, Kim *et al.* 2008, Hwang *et al.* 2009), compressive strength (Saliba *et al.* 2009), cytotoxicity and genotoxicity (Zeferino *et al.* 2010). In fact, those studies reported adequate solubility, setting time, pH and calcium ion release values (Vivan *et al.* 2010). In addition, one study showed that Portland cement and Portland cement with Bi_2O_3 had similar effects on the mineralization of human dental pulp cells (Min *et al.* 2009).

The addition of Bi_2O_3 to other types of MTA-like cements has also been studied. Dicalcium silicate cement containing 20 wt% Bi_2O_3 had a significantly longer setting time, probably as a result of the adverse effect of Bi_2O_3 on cement hardening; however, this was still considered adequate and shorter than that of White ProRoot MTA (Chiang & Ding 2010). Formosa *et al.* (2012) reported that Bi_2O_3 drastically increased setting time and advised further investigations with alternative radiopacifiers.

Radiopacifiers such as gold and silver/tin alloy added to Portland cement were considered suitable substitutes for Bi_2O_3 by Camilleri (2010a), as their chemical characteristics and physical properties were similar to those of ProRoot MTA. Other radiopacifying agents, such as calcium tungstate and zirconium oxide, have also been considered potential radiopacifiers in combination with Portland cement (Hungaro Duarte *et al.* 2012). Portland cement replaced with 30% zirconium oxide mixed at a water/cement proportion of 0.3 had optimal properties, similar to those of ProRoot MTA (Cutajar *et al.* 2011). In another study, the same research group investigated the hydration characteristics of 30% zirconium oxide in Portland cement and reported that it acted as an inert filler and did not react with the hydration by-products of Portland cement (Camilleri *et al.* 2011a).

Despite the hypothesis that Bi_2O_3 negatively affects the physical properties and chemical characteristics of MTA-like and Portland cements, there is insufficient evidence available regarding the precise effects of Bi_2O_3 on commercially available materials. Therefore, the aim of this study was to investigate the effects of the absence of Bi_2O_3 on White MTA Angelus using Rietveld X-ray diffraction analysis (XRD), energy-dispersive X-ray analysis (EDX), scanning electron microscopy (SEM), as well as compressive strength, Vickers microhardness and setting time. The null hypothesis was that White MTA Angelus and White MTA Angelus without Bi_2O_3 have the same chemical characteristics and physical properties.

Materials and methods

Sample preparation

The two materials investigated were (i) commercially available White MTA Angelus (Angelus Dental Industry Products S/A), composed of Bi_2O_3 added to Portland cement clinker (group 1), and (ii) White MTA Angelus without Bi_2O_3 (Angelus Dental Industry Products S/A), not commercially available, provided by the manufacturer (group 2).

Mixing of the materials was standardized by placing 1 g of either type of MTA and 0.33 g of distilled water in a plastic mixing capsule using a plastic pestle to facilitate mechanical agitation (Nekoofar *et al.* 2010a). The plastic capsules were immediately sealed, loaded into a ProMix™ amalgamator (Dentsply Caulk, York, PA, USA) and vibrated at 4500 revolutions per min for 30 s. The slurry was inserted in prefabricated cylindrical silicone moulds (Elite Double 22; Zhermack SpA, Rome, Italy) with dimensions that varied according to the test: (i) compressive strength, 6 ± 0.1 mm length and 4 ± 0.1 mm internal diameter, (ii) Vickers microhardness test, 1.5 ± 0.1 mm length and 5 ± 0.1 mm internal diameter, and (iii) setting time, 2 ± 0.1 mm length and 10 ± 0.1 mm internal diameter. For XRD and EDX, the hydrated

material was inserted in moulds with dimensions similar to those used for the compressive strength test.

The MTA slurries inside the moulds were then subjected to a constant vertical compaction force of 3.22 MPa applied for 1 min (Nekoofar *et al.* 2007). Then, the moulds were placed onto a damp paper towel in a sealed plastic container and incubated at 37 °C and 95% humidity for 7 days.

Rietveld XRD analysis

Both the dry powders (G1-powder and G2-powder) and the hydrated (G1-hydrated and G2-hydrated) forms of the material (2 g each group) were subjected to Rietveld XRD analysis. One sample of each form was analysed. The hydrated material was crushed to a fine powder before analysis (Formosa *et al.* 2012). Phase compositions of MTA specimens from each group were determined using an X-ray diffractometer (PANalytical X'Pert PRO, Almelo, the Netherlands) and CuKa radiation (40 Kv and 40 mA). Scans were undertaken in the 10–80° 2θ range. To identify crystalline compounds, all patterns were matched using the database of the International Centre for Diffraction Data (ICDD, Pennsylvania, PA, USA). The Rietveld refinement tool was used for the quantitative analysis of phases.

SEM and EDX analysis

Approximately 2 g of each hydrated material (one sample of each group) was used. After removing the samples from the incubator, their external surfaces were polished using the Metallic Backed Polishing Cloth System (Kemet, Maidstone, UK). They were then placed in an oven to dry at 60 °C for 24 h and subsequently in a vacuum chamber. Afterwards, samples were mounted on aluminium stubs using adhesive carbon discs and analysed uncoated, as previously described (Nekoofar *et al.* 2011, Formosa *et al.* 2012), using a scanning electron microscope (Carl Zeiss EVO 40, Oberkochen, Germany) fitted with an energy-dispersive X-ray detector (Oxford Instruments, Oxford, UK). Surface characteristics of the specimens in each group were examined and subjected to elemental analysis. Image locations were selected at random. EDX spectroscopy quantitatively and qualitatively determined the component elements using backscattered and secondary electrons (BSE and SE, respectively).

Chemical analysis (Rietveld XRD, SEM and EDX) was not performed in duplicate.

Compressive strength

Approximately 4 g of each material was used. After removal from the incubator, sample surfaces were polished with 1200-grit fine-grain sandpaper (Buehler-Met®; Agar Scientific Limited, Cambridge, UK). MTA samples were removed from the moulds and visually inspected to ensure that no voids or flaws were present before the test (G1, $n = 15$; G2, $n = 12$). The test was performed in accordance with ISO 9917-1:2003 standards, using a universal testing machine (Lloyd LR MK1; Lloyd Instruments, Fareham, UK) in which a calibrated steel cross-head plate moved at 1 mm min^{-1}. When both planes were in contact with the samples, the compressive load was recorded in MPa until failure.

Vickers microhardness

Approximately 4 g of each material was used, with ten samples in each group. After removal from the incubator, surfaces were polished using 600, 1000 and 1200-grit fine-grain sandpapers (Buehler-Met®; Agar Scientific Limited), to obtain flat surfaces. The test followed the European and British Standard (BS EN 843-4:2005) and used a Micromet 5114 tester (Buehler Ltd, Lake Bluff, IL, USA) with a square-based pyramid-shaped diamond indenter and a full load of 1000 g for 30 s at room temperature. This produced a quadrangular depression with two equal orthogonal diagonals in the polished surface of the cement. One trained operator performed seven randomly placed indentations on each sample. The two diagonals produced were measured immediately under the microscope, and the Vickers surface microhardness value displayed on the digital readout of the tester was recorded in MPa.

Setting time

Approximately 4 g of each material was used, with six samples in each group. Two previously trained operators measured the initial and final setting times of all samples in accordance with the American Society for Testing and Materials (ASTM) International Standard C266-08 (2008) and the American National Standards Institute/American Dental Association (ANSI/ADA) Specification No. 57 (2008). The test was performed at 37 °C inside an incubator (all test equipment was placed and maintained in an incubator at all times in-between measurements) using a

Gillmore apparatus CT-5 (ELE International Inc., Loveland, CO, USA). The apparatus included two needles: the needle for testing the initial setting time, which weighed 113.4 g and had a 2.12-mm diameter tip, and the needle for the final setting time, which weighed 453.6 g and had a 1.06-mm tip.

Incubation times prior to the initial and the final setting time tests were determined in a pilot study. White MTA Angelus samples were incubated immediately after hydration for 10 min. After the completion of the initial setting time test and before the start of the final setting time test, samples were incubated for an additional 45 min. White MTA without Bi_2O_3 specimens were incubated for 5 and 30 min, respectively.

The initial needle was applied lightly on the surface of each sample. The procedure was repeated every 60 s until the needle did not create a complete circular depression on the specimen surface. For each sample, the time elapsed between the end of mixing and unsuccessful indentation was recorded in minutes and defined as the initial setting time. The final setting time was determined following the same procedures using the second needle.

Data analysis

The Rietveld XRD was used to semi-quantitatively identify and quantify the main phases related to the MTA hydration process: tricalcium silicate (Ca_3SiO_5), dicalcium silicate (Ca_2SiO_4), calcium hydroxide ($CaOH_2$), ettringite (E), bismuth oxide (Bi_2O_3) and tricalcium aluminate ($Ca_3Al_2O_6$). These data were analysed descriptively (%).

Energy-dispersive X-ray analysis was used to identify essential compounds of the sample, such as calcium, aluminium, bismuth, silicon and sulphur. SEM images obtained from White MTA Angelus and White MTA Angelus without Bi_2O_3 were compared for the presence of bismuth, silicon, and calcium and also with regard to sample surface morphology: porosity, acicular crystals, spiky ball-like clusters and globular formations. These data were also analysed descriptively (%).

Compressive strength and surface microhardness data were compared using the Student's *t*-test, and the setting time data using the Mann–Whitney U test (Statistical Package for the Social Sciences version 17.0 for Windows; SPSS Inc, Chicago, IL, USA). Statistical significance was set at $P < 0.05$.

Results

Rietveld XRD analysis

X-ray diffraction patterns in the 10–80° 2θ range and Rietveld analysis results are shown in Figs 1–4. Diffractograms revealed several unidentifiable peaks in White MTA Angelus powder (Fig. 1), for instance at 43.3, 44.56, 47.73 and 50.73°, probably as a result of their high θ values. These peaks may characterize a single amorphous phase or a combination of phases with low crystallinity, and therefore, they were not included in the Rietveld XRD analysis (semi-quantitative analysis).

Overall, both types of MTA revealed tricalcium silicate and dicalcium silicate. A reduction in tricalcium silicate peaks was observed in the diffractograms of the two hydrated forms (Figs 2 and 4) when

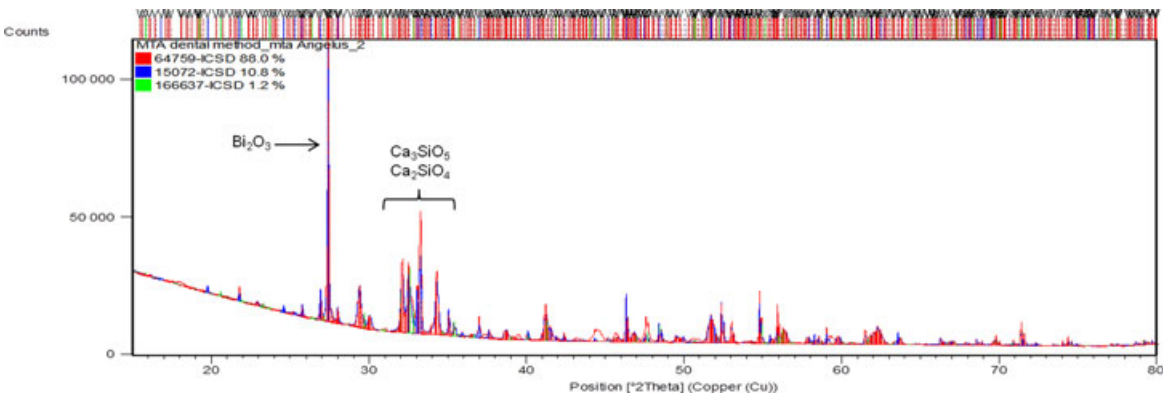

Figure 1 White mineral trioxide aggregate (MTA) Angelus, powder form (G1-powder): diffractogram showing tricalcium silicate (Ca_3SiO_5), dicalcium silicate (Ca_2SiO_4) and bismuth oxide (Bi_2O_3) peaks; Rietveld analysis showing 88.0% Ca_3SiO_5 [64759], 10.8% Bi_2O_3 [15072] and 1.2% Ca_2SiO_4 [166637].

compared with the powder forms (Figs 1 and 3); this finding was confirmed in the Rietveld analysis. Calcium hydroxide was present in the two hydrated forms (Figs 2 and 4). According to the Rietveld analysis, the hydrated forms were associated with a large amount of amorphous phase. White MTA Angelus without Bi_2O_3 powder contained an aluminate phase ($Ca_9Al_6O_{18}{\cdot}26H_2O$ [1841]) in Rietveld analysis, with a diffractogram peak at 30–35° 2θ (*N*) (Fig. 3). The diffractogram of hydrated White MTA Angelus without Bi_2O_3 revealed a small ettringite peak (Fig. 4). Bi_2O_3 peaks were present in diffractograms of White MTA Angelus, but not in White MTA Angelus without Bi_2O_3. In hydrated White MTA Angelus, Bi_2O_3 peak intensity at 27.30° 2θ was slightly lower than in White MTA Angelus powder (Figs 1 and 2).

EDX and SEM analysis

Hydrated White MTA (G1-hydrated)

The characterization obtained for White MTA after 7 days of hydration is described. In EDX analysis,

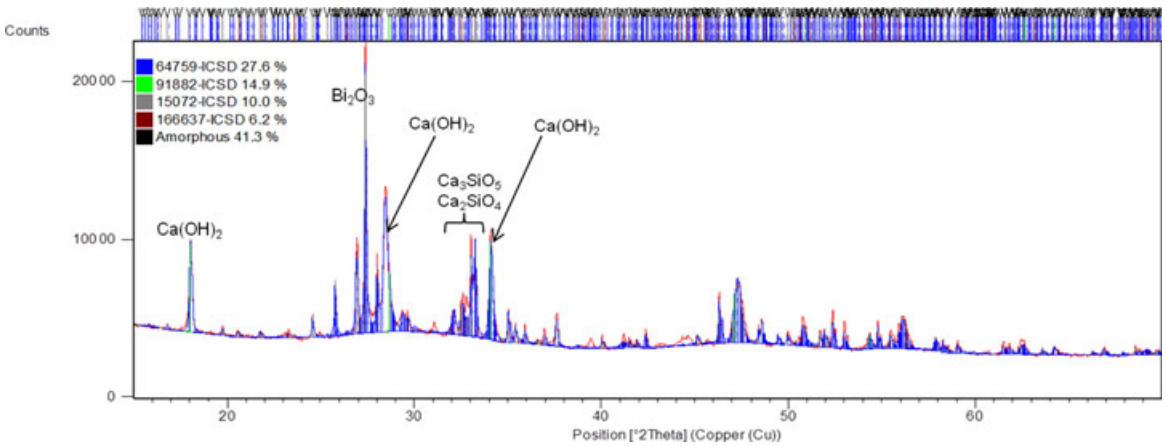

Figure 2 White mineral trioxide aggregate (MTA) Angelus, hydrated form (G1-hydrated): diffractogram showing tricalcium silicate (Ca_3SiO_5), dicalcium silicate (Ca_2SiO_4), bismuth oxide (Bi_2O_3) and calcium hydroxide ($Ca[OH]_2$) peaks; Rietveld analysis showing 41.3% amorphous phase, 27.6% Ca_3SiO_5 [64759], 14.9% $Ca(OH)_2$ [91882], 10% Bi_2O_3 [15072] and 6.2% Ca_2SiO_4 [166637].

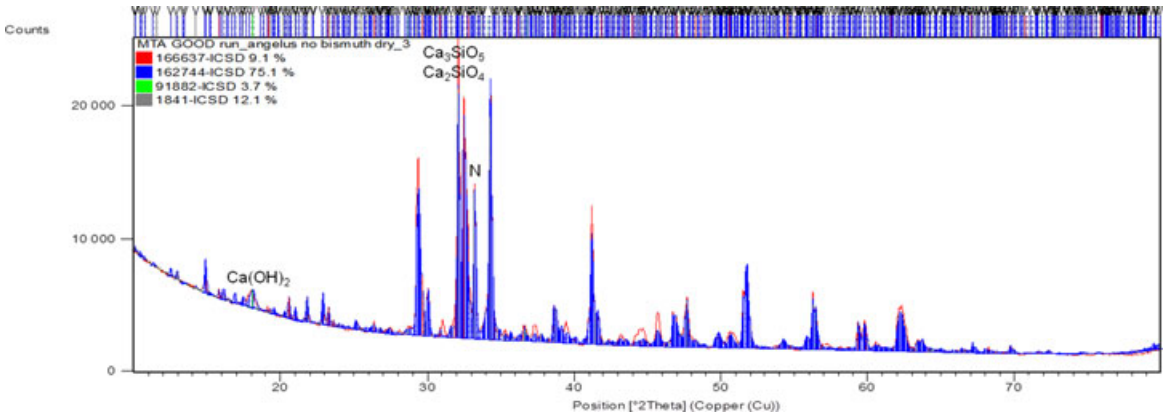

Figure 3 White mineral trioxide aggregate (MTA) Angelus without Bi_2O_3, powder form (G2-powder): diffractogram showing tricalcium silicate (Ca_3SiO_5), dicalcium silicate (Ca_2SiO_4), calcium hydroxide ($Ca[OH]_2$) and calcium hexa-aluminate ($Al_6Ca_9O_{18}$[N]) peaks; Rietveld analysis showing 75.1% Ca_3SiO_5 [162744], 12.1% $Ca_9AL_6O_{18}{\cdot}26H_2O$ [1841], 9.1% Ca_2SiO_4 [166637] and 3.7% $Ca(OH)_2$ [91882].

X-rays are distributed over the spectrum in relation to their energy, most commonly from the lowest to the highest atomic number (low energy to high energy). Figure 5 shows the results of the qualitative (a) and quantitative (b) analyses carried out, including the presence of bismuth. Figure 6 shows surface characteristics based on secondary electron (SE) images obtained at 653× (a), 2.61× (b), 5.00× (c) and 1454× (d) magnifications, in addition to one backscattered (BSE) image obtained at 1.23× (e) magnification.

Hydrated White MTA without Bi_2O_3 (G2-hydrated)

The results obtained for the White MTA formulation without Bi_2O_3 after 7 days of hydration are described. Figure 7 shows the results of qualitative (a) and quantitative (b) analyses of the tested material. Bismuth and iron were not detected. Figure 8 shows surface characteristics based on secondary electron (SE) images obtained at 1.95× (a), 935× (b) and 653× (c) magnification, in addition to one backscattered (BSE) image obtained at 1.23× (d) magnification.

Compressive strength, Vickers microhardness and setting time

The results obtained for these variables in both materials are shown in Table 1. The statistical analysis showed significant differences ($P < 0.05$) between groups for Vickers microhardness test (White MTA Angelus = 39 964.07 MPa, White MTA Angelus without Bi_2O_3 = 35 909.33 MPa) and for final setting time (White MTA Angelus = 165 min, White MTA Angelus without Bi_2O_3 = 38.33 min).

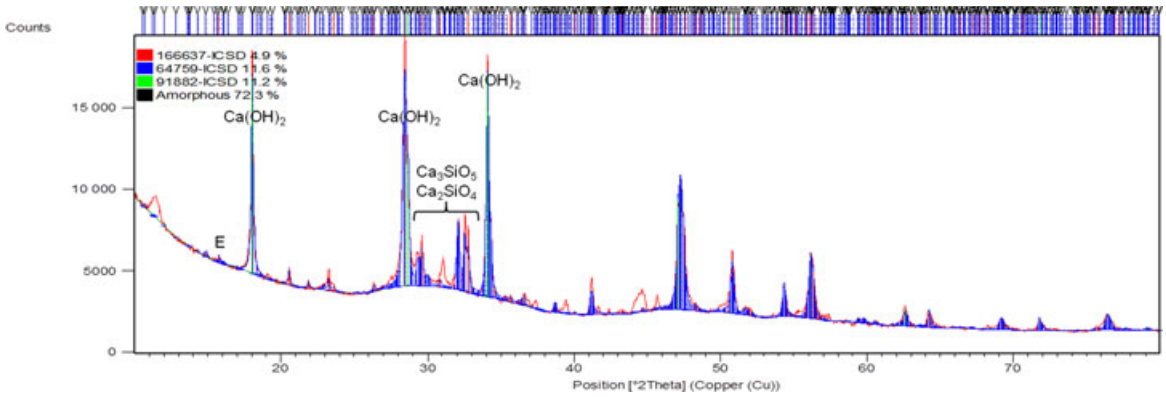

Figure 4 White mineral trioxide aggregate (MTA) Angelus without Bi_2O_3, hydrated form (G2-hydrated): diffractogram showing tricalcium silicate (Ca_3SiO_5), dicalcium silicate (Ca_2SiO_4) and calcium hydroxide ($Ca[OH]_2$) peaks, plus a small peak for $(SO_4)(OH)_{12}\cdot 26H_2O$ (ettringite-E); Rietveld analysis showing 72.3% amorphous phase, 11.6% Ca_3SiO_5 [64759], 11.2% $Ca(OH)_2$ [91882] and 4.9% Ca_2SiO_4 [166637].

(a)

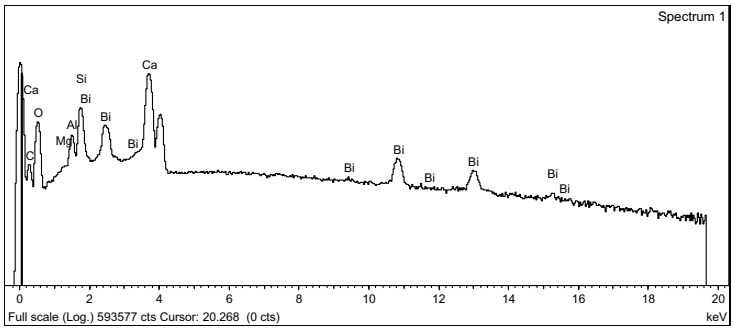

(b)

Element	Weight%
C K	2.62
O K	42.69
Mg K	0.08
Al K	1.48
Si K	6.08
Ca K	40.24
Bi M	6.81
Total	100.00

Figure 5 Energy-dispersive X-ray analysis (EDX) spectrum (total area) for hydrated White mineral trioxide aggregate (MTA) Angelus (a) and weight (%) of constituent elements (b).

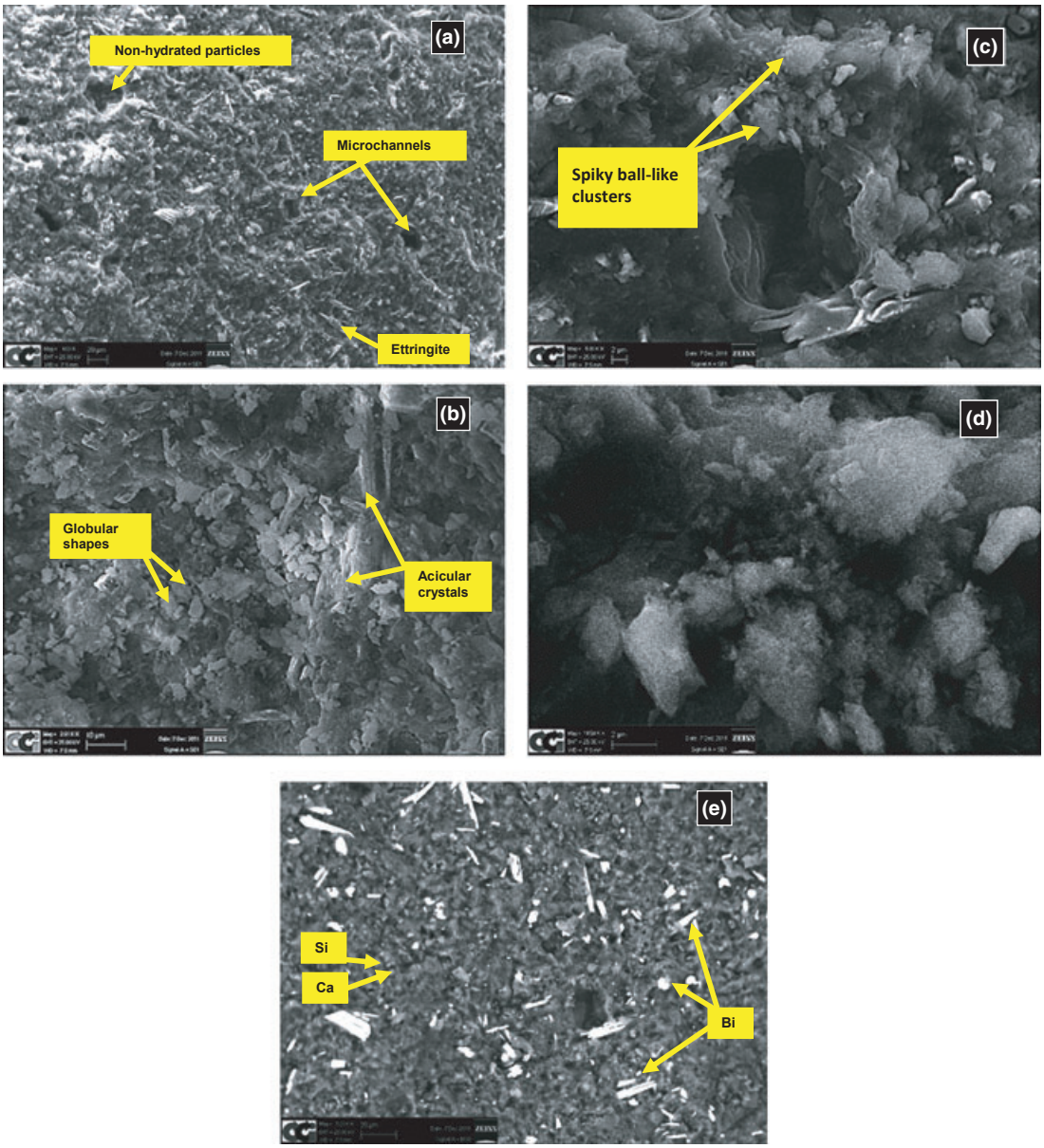

Figure 6 Scanning electron microscopy (secondary electron) images (a, b, c, d) obtained from hydrated White mineral trioxide aggregate (MTA) Angelus showing the presence of nonhydrated particles (a), ettringite (a) and microchannels (a). Ettringite is characterized by acicular crystal formation, evidenced as long spanning forms (b) as well as spiky ball-like clusters (c, d). Some globular formations were also observed (b). The backscattered electron image (e) shows the presence of bright particles, that is, bismuth (Bi), supported upon a calcium silicate matrix: silicon (Si) corresponds to the darker grey and calcium (Ca) to the lighter grey.

Discussion

The effects of Bi_2O_3 on MTA-like and Portland cements have been associated with chemical alterations and deterioration of physical properties (Coomaraswamy *et al.* 2007, Camilleri 2008a, Chiang & Ding 2010, Formosa *et al.* 2012), which has motivated the investigation of alternative radiopacifiers (Camilleri 2010a,b, Camilleri *et al.* 2011a, Cutajar *et al.* 2011, Hungaro Duarte *et al.* 2012). The aim of the present study was to assess the effects of Bi_2O_3 present in commercially available White MTA (Angelus) and of its absence in a

(a)

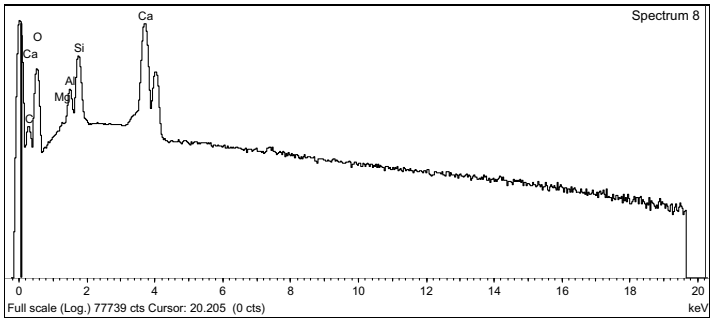

(b)

Element	Weight%
C K	2.48
O K	52.88
Mg K	0.14
Al K	1.74
Si K	7.60
Ca K	35.17
Total	100.00

Figure 7 Energy-dispersive X-ray analysis (EDX) spectrum (total area) for hydrated White mineral trioxide aggregate (MTA) Angelus without Bi_2O_3 (a) and weight (%) of constituent elements (b).

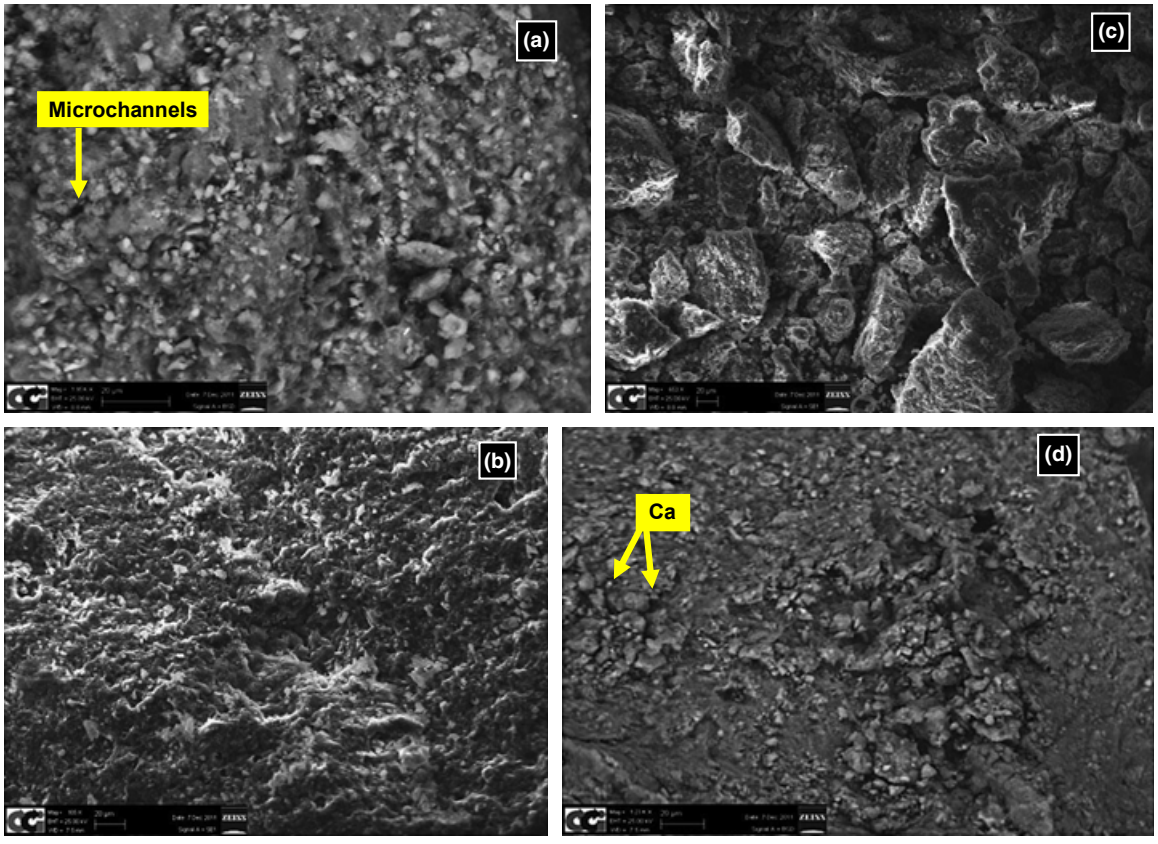

Figure 8 Scanning electron microscopy (secondary electron) images (a, b, c) obtained from hydrated White mineral trioxide aggregate (MTA) Angelus without Bi_2O_3 showing a different structure from hydrated White MTA Angelus. Secondary electron images (a, b) did not reveal acicular crystals or spiky ball-like clusters (characteristic of ettringite – hexacalcium aluminate trisulphate hydrate). The absence of bright particles (bismuth) and the presence of crystals with well-defined edges were also evident (c), a characteristic formation of calcium hydroxide $Ca(OH)_2$. The backscattered electron image shows a large amount of calcium (d).

unique White MTA formulation without Bi_2O_3 (Angelus).

Results revealed that the lack of Bi_2O_3 had an influence on several properties of MTA after 7 days of hydration: chemical and morphological analyses (Rietveld XRD, EDX and SEM) revealed differences in chemical characterization between White MTA Angelus and White MTA Angelus without Bi_2O_3; physical

Table 1 Compressive strength (MPa), Vickers microhardness (MPa) and setting time (min) for White mineral trioxide aggregate(MTA) Angelus and White MTA Angelus without Bi_2O_3

		Group	*N*	Mean	Standard deviation	Hypothesis test, *P*
Compressive strength (MPa)		White MTA Angelus	15	39 964.07	10 503.680	0.329*
		White MTA Angelus without Bi_2O_3	12	35 909.33	10 546.706	
Vickers microhardness (MPa)		White MTA Angelus	10	47.87	6.365	0.000*
		White MTA Angelus without Bi_2O_3	10	72.35	9.515	
Setting time (min)	Initial	White MTA Angelus	6	18.33	7.528	0.061**
		White MTA Angelus without Bi_2O_3	6	10.00	0.000	
	Final	White MTA Angelus	5	165.00	31.623	0.002**
		White MTA Angelus without Bi_2O_3	6	38.33	9.832	

*Student's *t*-test, **Mann–Whitney U test, $\alpha = 0.05$.

tests revealed the influence of Bi_2O_3 on setting time and a reduction in Vickers microhardness values. Compressive strength, in turn, was not affected.

Rietveld XRD analysis is able to identify the crystalline phases of cements (Camilleri 2008b, Shokouhinejad *et al.* 2012), but not amorphous structures. Diffraction patterns provide information on the chemical characterization of cements, which is relevant to the understanding of the material's performance (Camilleri 2008b).

Tricalcium silicate and dicalcium silicate, that is, the main crystalline phases involved in the hydration of MTA (Camilleri *et al.* 2005a, Islam *et al.* 2006b, Camilleri 2008b, Belío-Reyes *et al.* 2009), were detected in the Rietveld XRD analysis. It has already been reported that tricalcium silicate is one of the main phases present in nonhydrated cements, accounting for a large portion of the MTA (Islam *et al.* 2006b, Camilleri 2008b, Belío-Reyes *et al.* 2009) and Portland cement powder (Camilleri *et al.* 2005b, Camilleri 2008b, 2011b). The percentage of calcium silicate will depend on the type of cement and on the manufacturing process (Neville 2000).

Similarly to Camilleri (2008b) and Belío-Reyes *et al.* (2009), a large proportion of calcium silicate in relation to other phases was observed in both powders investigated. Nevertheless, the real percentage of this compound was not calculated due to the presence of several noncharacterized peaks resulting from an amorphous phase or a combination of phases with low crystallinity. According to Camilleri (2008b), a solution to this problem would be the use of internal reference patterns in the XRD analysis that would allow the identification and quantification of amorphous phases.

The reduced amount of calcium silicate found in the hydrated forms of the two materials when compared with the respective powders is in agreement with the study of Camilleri (2008b). Such reduction is a consequence of the hydration of calcium silicate, which begins soon after powder and water are combined and produces calcium hydroxide ($Ca[OH]_2$) and calcium silicate hydrate gel (C-S-H) (Zhao *et al.* 2005, Gandolfi *et al.* 2010). C-S-H gel is included in the amorphous phase, which was detected in large amounts in the analysis of hydrated cements in the present study. This gel does not produce well-defined peaks because it is part of a noncrystalline phase (Camilleri 2007, 2008b). According to Torabinejad *et al.* (1995) and Asgary *et al.* (2009), MTA has both phases after hydration: a crystalline and an amorphous phase. Cavenago *et al.* (2013) studied MTA manipulated with different amounts of distilled water. Based on the findings of that study, it is possible to conclude that increases in the amorphous phase have an effect increasing the contact (contact surface) between the aqueous medium and the material, accelerating material dissolution and consequently increasing calcium release. Notwithstanding, mechanical properties are usually not affected, as the amorphous phase tends to increase material rigidity and hardness.

In the present study, the presence of $Ca(OH)_2$ in the two hydrated formulations confirms that finding. The presence of $Ca(OH)_2$ in the powder form of White MTA without Bi_2O_3, as revealed in the Rietveld XRD analysis, was unexpected.

The aluminate phase present in the powder formulation of White MTA without Bi_2O_3 may be associated with the low ettringite peaks observed in this diffractogram after hydration. Ettringite is a crystalline complex resulting from hydration of the aluminate phase. It contains calcium, aluminium, silicon and sulphur (Camilleri *et al.* 2005b). This compound is characterized by an acicular crystal network (needlelike crystals), responsible for resistance and hardening in early hydration stages (Camilleri 2007). Therefore, in

White MTA Angelus without Bi_2O_3, even though aluminate and ettringite phases were detected in the Rietveld XRD analysis, the surface morphology observed on SEM did not include acicular crystal formations. Unlike White MTA Angelus without Bi_2O_3, in White MTA with Bi_2O_3, aluminate and ettringite phases could not be detected in the Rietveld XRD analysis. Nevertheless, it is interesting to note that the corresponding SEM images revealed long spanning forms and spiky ball-like clusters.

The partial inability of the two experimental methods to detect ettringite may be a consequence of the reduced amounts of aluminate phase, as evidenced in both groups. Camilleri (2007) has also reported that the reduction or absence of the aluminate phase led to no ettringite production, a characteristic that has been observed in recently developed MTA-like cements, resulting in biological improvements (De-Deus *et al.* 2009).

The absence of bismuth in White MTA Angelus without Bi_2O_3 was verified by both Rietveld XRD and EDX/SEM analyses. In White MTA Angelus, Rietveld XRD revealed a low amount of Bi_2O_3 in the hydrated cement in relation to the powder form, a finding that has been reported previously (Camilleri 2007, 2008b, 2010a). According to those previous studies, Bi_2O_3 in MTA is not inert, unlike other radiopacifiers that work as fillers in the cement hydration process (Camilleri 2010a). Rather, Bi_2O_3 has been reported to be part of the hydrated phase, forming a structure comprised of calcium silicate bismuth hydrate (C-S-H-Bi); it also affects $Ca(OH)_2$ precipitation in the hydrated material. This fact could interfere with the bioactivity of the material.

Camilleri (2007) reported a reduction in the precipitation of calcium hydroxide in hydrated MTA when compared with a Portland cement with no Bi_2O_3. Unbound bismuth leaches into surrounding tissues (together with calcium hydroxide formed from the hydration of calcium silicates), at increasing amounts over time. In the present study, SEM (backscattered) images obtained from White MTA Angelus revealed the presence of bismuth. Surface morphology analysis suggested that bismuth was within the bulk of the material and was also located on its surface, possibly manifested as unbound bismuth particles.

Moreover, the possibility that $Ca(OH)_2$ precipitation in White MTA Angelus was affected by the participation of bismuth in hydration mechanisms is supported by the comparison of diffractograms obtained for the two hydrated formulations (White MTA Angelus without Bi_2O_3 diffractometer peaks were higher than those of White MTA Angelus) and also by SEM (ES) images: in contrast to White MTA Angelus specimens, SEM images obtained for White MTA Angelus without Bi_2O_3 showed crystals with well-defined edges (Fig. 8d) and a morphology characteristic of $Ca(OH)_2$, as already shown in the study of Formosa *et al.* (2012).

The presence of microchannels was confirmed in the SEM images acquired for both groups. These microchannels are interconnected with a network of small pores and are critical for a complete formation of the crystalline phase (Hewlett 2004) and for the progression of the hydration process (Fridland & Rosado 2003, Nekoofar *et al.* 2007).

Compressive strength is important when MTA is used as a base material, in the repair of furcal perforations (Islam *et al.* 2006a). According to manufacturer's information, the compressive strength of MTA Angelus is 40 MPa after 24 h of hydration; similar values were found in this study: 39.9 MPa for White MTA Angelus and 35.9 for White MTA Angelus without Bi_2O_3 after 7 days of hydration. A correlation between low compressive strength and absence of acicular crystals has been reported (Lee *et al.* 2004, Kayahan *et al.* 2009, Nekoofar *et al.* 2010b,c) in cements subjected to acid-etching and blood contamination. In the present study, suitable compressive strength values were observed for both cement types, without a significant difference between them. Evidence of crystalline structures was also found in both groups: White MTA Angelus (on EDX/SEM) and White MTA Angelus without Bi_2O_3 (aluminate phase and ettringite peaks on Rietveld XRD). It can therefore be inferred that Bi_2O_3 did not affect the compressive strength of the material. Other authors have also reported that the addition of varying percentages of Bi_2O_3 did not influence the physical properties of Portland cement (Saliba *et al.* 2009). Conversely, in some studies, Bi_2O_3 was found to reduce compressive strength when added to Portland cement (Coomaraswamy *et al.* 2007, Camilleri 2008a). This variation in the results reported by different studies is influenced by many factors, for example, water/powder ratio, size and shape of samples, sample preparation, and hydration time. In addition, condensation pressure (i.e. when the material is inserted into the mould) has also been shown to affect the physical properties (strength and hardness) of MTA (Nekoofar *et al.* 2007). For this reason, the present study used a standardized, controlled compression force, as suggested by Nekoofar *et al.* (2007).

After 7 days of hydration, White MTA Angelus without Bi_2O_3 had significantly higher mean values on the Vickers microhardness test than White MTA Angelus (72.35 MPa vs. 47.87 MPa). There is no evidence in the literature regarding the influence of Bi_2O_3 on Vickers microhardness results for MTA, Portland or MTA-like cements. Several recent publications focusing on Vickers microhardness of ProRoot MTA took a number of confounding factors into consideration, for example, blood contamination (Nekoofar *et al.* 2010c), mixing techniques (Nekoofar *et al.* 2010a), environmental pH (Giuliani *et al.* 2010), humidity (Kang *et al.* 2012) and cement nanomodification (Saghiri *et al.* 2012). The study of Nekoofar *et al.* (2010c) reported a mean MPa value of 59.91 ± 5.72 for surface microhardness of White ProRoot MTA after 4 days of hydration in distilled water. Based on these considerations, it seems that the two groups (White MTA Angelus and White MTA Angelus without Bi_2O_3) had suitable Vickers microhardness mean values, possibly related to the amount of amorphous phase (Sestak *et al.* 2010) observed on Rietveld XRD for the two hydrated forms. The lower mean values obtained in White MTA Angelus may be explained by the presence of unbound bismuth.

Both compressive strength and surface hardness are indicators of the setting process (Lee *et al.* 2004, Camilleri 2007, 2008a, Nekoofar *et al.* 2007), with interconnected, mutually complementary physicochemical properties (Vivan *et al.* 2010). Cements with long setting times are potentially more susceptible to dissolution and wash-out during endodontic surgery, whereas extremely short setting times may pose technical difficulties during clinical application (Vivan *et al.* 2010). The literature reports initial and final setting times of 40 and 140 min, respectively, for ProRoot MTA (Chng *et al.* 2005, Islam *et al.* 2006a). These values are different from those previously reported for MTA Angelus: 10 and 15 min (http://www.angelus.ind.br), 12 and 48 min (Bortoluzzi *et al.* 2009), and 9.33 and 23.33 min (Vivan *et al.* 2010). In the present study, initial and final setting times were 18.33 and 165 min for White MTA Angelus and 10 and 38.33 for White MTA Angelus without Bi_2O_3, respectively.

Mean initial setting time for White MTA was longer than for White MTA without Bi_2O_3. However, statistical analysis did not show any differences between groups. In fact, as the P value ($P = 0.061$) was close to 0.05, there is the possibility that a larger sample size could yield differences. Bi_2O_3 present in White MTA Angelus was associated with a significantly longer final setting time in relation to White MTA Angelus without Bi_2O_3 ($P = 0.002$). Other reports have demonstrated that Bi_2O_3 retards setting when added to Portland cement (Camilleri 2010a, Formosa *et al.* 2012, Hungaro Duarte *et al.* 2012) and MTA-like cements (Chiang & Ding 2010, Formosa *et al.* 2012). A reduced amount of C-S-H in hydrated materials containing Bi_2O_3 will produce a poorer and slower hydration reaction, resulting in a longer setting time (Chen *et al.* 2009). In this regard, Chiang and Ding (2010) reported that when Bi_2O_3 is added to MTA-like cements, a smaller liquid/powder ratio is needed. This radiopacifier does not act as a filler; thus, a smaller amount of water is sufficient to hydrate the powder. Future studies with larger volumes of water to hydrate MTA-like cements without Bi_2O_3 are suggested.

Conclusions

Bi_2O_3 was associated with modifications in the chemical characterization and physical properties of White MTA Angelus, as follows:

- Rietveld XRD analysis suggested similar behaviours for the two groups [reduction of tricalcium silicate and detection of $Ca(OH)_2$ after hydration].
- SEM images revealed important differences, for example, bismuth particles located on the material surface for White MTA Angelus and amorphous particles characteristic of $Ca(OH)_2$ for White MTA Angelus without Bi_2O_3.
- White MTA Angelus without Bi_2O_3 showed a shorter final setting time, higher Vickers microhardness mean values and similar compressive strength mean values when compared with White MTA Angelus.

Acknowledgement

The authors acknowledge the financial assistance from CAPES (Process number 6904-10-6), which enabled Renata Grazziotin-Soares to hold a Visiting Research Fellow at the Cardiff University School of Dentistry.

References

von Arx T, Jensen SS, Hänni S, Friedman S (2012) Five-year longitudinal assessment of the prognosis of apical microsurgery. *Journal of Endodontics* **38**, 570–9.

Asgary S, Eghbal MJ, Parirokh M, Ghoddusi J, Kheirieh S, Brink F (2009) Comparison of mineral trioxide aggregate's composition with Portland cements and a new endodontic cement. *Journal of Endodontics* **35**, 243–50.

Belío-Reyes IA, Bucio L, Cruz-Chavez E (2009) Phase composition of ProRoot mineral trioxide aggregate by X-ray powder diffraction. *Journal of Endodontics* **35**, 875–8.

Bernabé PF, Gomes-Filho JE, Cintra LT *et al.* (2010) Histologic evaluation of the use of membrane, bone graft, and MTA in apical surgery. *Oral Surgery Oral Medicine Oral Pathology Oral Radiology and Endodontics* **109**, 309–14.

Bortoluzzi EA, Broon NJ, Bramante CM, Felippe WT, Tanomaru Filho M, Esberard RM (2009) The influence of calcium chloride on the setting time, solubility, disintegration, and pH of mineral trioxide aggregate and white Portland cement with a radiopacifier. *Journal of Endodontics* **35**, 550–4.

Camilleri J (2007) Hydration mechanisms of mineral trioxide aggregate. *International Endodontic Journal* **40**, 462–70.

Camilleri J (2008a) The physical properties of accelerated Portland cement for endodontic use. *International Endodontic Journal* **41**, 151–7.

Camilleri J (2008b) Characterization of hydration products of mineral trioxide aggregate. *International Endodontic Journal* **41**, 408–17.

Camilleri J (2010a) Evaluation of the physical properties of an endodontic Portland cement incorporating alternative radiopacifiers used as root-end filling material. *International Endodontic Journal* **43**, 231–40.

Camilleri J (2010b) Hydration characteristics of calcium silicate cements with alternative radiopacifiers used as root-end filling materials. *Journal of Endodontics* **36**, 502–8.

Camilleri J (2011b) Characterization and hydration kinetics of tricalcium silicate cement for use as a dental biomaterial. *Dental Materials* **27**, 836–44.

Camilleri J, Gandolfi MG (2010) Evaluation of the radiopacity of calcium silicate cements containing different radiopacifiers. *International Endodontic Journal* **43**, 21–30.

Camilleri J, Montesin FE, Brady K, Sweeney R, Curtis RV, Ford TR (2005a) The constitution of mineral trioxide aggregate. *Dental Materials* **21**, 297–303.

Camilleri J, Montesin FE, Di Silvio L, Pitt Ford TR (2005b) The chemical constitution and biocompatibility of accelerated Portland cement for endodontic use. *International Endodontic Journal* **38**, 834–42.

Camilleri J, Cutajar A, Mallia B (2011a) Hydration characteristics of zirconium oxide replaced Portland cement for use as a root-end filling material. *Dental Materials* **27**, 845–54.

Camilleri J, Kralj P, Veber M, Sinagra E (2012) Characterization and analyses of acid extractable and leached trace elements in dental cements. *International Endodontic Journal* **45**, 737–43.

Cavenago BC, Pereira TC, Duarte MA *et al.* (2013) Influence of powder-to-water ratio on radiopacity, setting time, pH, calcium ion release and a micro-CT volumetric solubility of white mineral trioxide aggregate. *International Endodontic Journal* doi: 10.1111/iej.12120. [Epub ahead of print].

Chen CC, Ho CC, David Chen CH, Ding SJ (2009) Physicochemical properties of calcium silicate cements for endodontic treatment. *Journal of Endodontics* **35**, 1288–91.

Chiang TY, Ding SJ (2010) Comparative physicochemical and biocompatible properties of radiopaque dicalcium silicate cement and mineral trioxide aggregate. *Journal of Endodontics* **36**, 1683–7.

Chng HK, Islam I, Yap AUJ, Tong YW, Koh ET (2005) Properties of a new root-end filling material. *Journal of Endodontics* **31**, 665–8.

Chong BS, Pitt Ford TR, Hudson MB (2003) A prospective clinical study of mineral trioxide aggregate and IRM when used as root-end filling materials in endodontic surgery. *International Endodontic Journal* **36**, 520–6.

Coomaraswamy KS, Lumley PJ, Hofmann MP (2007) Effect of bismuth oxide radioopacifier content on the material properties of an endodontic Portland cement-based (MTA-like) system. *Journal of Endodontics* **33**, 295–8.

Coutinho-Filho T, De-Deus G, Klein L, Manera G, Peixoto C, Gurgel-Filho ED (2008) Radiopacity and histological assessment of Portland cement plus bismuth oxide. *Oral Surgery Oral Medicine Oral Pathology Oral Radiology and Endodontics* **106**, e69–77.

Cutajar A, Mallia B, Abela S, Camilleri J (2011) Replacement of radiopacifier in mineral trioxide aggregate; characterization and determination of physical properties. *Dental Materials* **27**, 879–91.

De-Deus G, Canabarro A, Alves G, Linhares A, Senne MI, Granjeiro JM (2009) Optimal cytocompatibility of a bioceramic nanoparticulate cement in primary human mesenchymal cells. *Journal of Endodontics* **35**, 1387–90.

Erdem AP, Guven Y, Balli B *et al.* (2011) Success rates of mineral trioxide aggregate, ferric sulfate, and formocresol pulpotomies: a 24-month study. *Pediatric Dentistry* **33**, 165–70.

Formosa LM, Mallia B, Camilleri J (2012) The effect of curing conditions on the physical properties of tricalcium silicate cement for use as a dental biomaterial. *International Endodontic Journal* **45**, 326–36.

Fridland M, Rosado R (2003) Mineral trioxide aggregate (MTA) solubility and porosity with different water-topowder ratios. *Journal of Endodontics* **29**, 814–7.

Gandolfi MG, Van Landuyt K, Taddei P, Modena E, Van Meerbeek B, Prati C (2010) Environmental scanning electron microscopy connected with energy dispersive x-ray analysis and Raman techniques to study ProRoot mineral trioxide aggregate and calcium silicate cements in wet conditions and in real time. *Journal of Endodontics* **36**, 851–7.

Giuliani V, Nieri M, Pace R, Pagavino G (2010) Effects of pH on surface hardness and microstructure of mineral trioxide aggregate and Aureoseal: an *in vitro* study. *Journal of Endodontics* **36**, 1883–6.

Hewlett PC (2004) *Lea's chemistry of cement and concrete*, 4th edn. Oxford, UK: Elsevier Butterworth Heinmann.

Hungaro Duarte MA, Minotti PG, Rodrigues CT *et al.* (2012) Effect of different radiopacifying agents on the physicochemical properties of white Portland cement and white mineral trioxide aggregate. *Journal of Endodontics* **38**, 394–7.

Hwang YC, Lee SH, Hwang IN *et al.* (2009) Chemical composition, radiopacity, and biocompatibility of Portland cement with bismuth oxide. *Oral Surgery Oral Medicine Oral Pathology Oral Radiology and Endodontics* **107**, e96–102.

Islam I, Chng HK, Yap AU (2006a) Comparison of the physical and mechanical properties of MTA and portland cement. *Journal of Endodontics* **32**, 193–7.

Islam I, Chng HK, Yap AU (2006b) X-ray diffraction analysis of mineral trioxide aggregate and Portland cement. *International Endodontic Journal* **39**, 220–5.

Kang JS, Rhim EM, Huh SY *et al.* (2012) The effects of humidity and serum on the surface microhardness and morphology of five retrograde filling materials. *Scanning* **34**, 207–14.

Kayahan MB, Nekoofar MH, Kazandag M *et al.* (2009) Effect of acid-etching procedure on selected physical properties of mineral trioxide aggregate. *International Endodontic Journal* **42**, 1004–14.

Kim EC, Lee BC, Chang HS, Lee W, Hong CU, Min KS (2008) Evaluation of the radiopacity and cytotoxicity of Portland cements containing bismuth oxide. *Oral Surgery Oral Medicine Oral Pathology Oral Radiology and Endodontics* **105**, e54–7.

Lee SJ, Monsef M, Torabinejad M (1993) Sealing ability of a mineral trioxide aggregate for repair of lateral root perforations. *Journal of Endodontics* **19**, 541–4.

Lee YL, Lee BS, Lin FH, Yun Lin A, Lan WH, Lin CP (2004) Effects of physiological environments on the hydration behavior of mineral trioxide aggregate. *Biomaterials* **25**, 787–93.

Lindeboom JA, Frenken JW, Kroon FH, van den Akker HP (2005) A comparative prospective randomized clinical study of MTA and IRM as root-end filling materials in single-rooted teeth in endodontic surgery. *Oral Surgery Oral Medicine Oral Pathology Oral Radiology and Endodontics* **100**, 495–500.

Mente J, Hage N, Pfefferle T *et al.* (2010) Treatment outcome of mineral trioxide aggregate: repair of root perforations. *Journal of Endodontics* **36**, 208–13.

Min KS, Lee SI, Lee Y, Kim EC (2009) Effect of radiopaque Portland cement on mineralization in human dental pulp cells. *Oral Surgery Oral Medicine Oral Pathology Oral Radiology and Endodontics* **108**, e82–6.

Nair PN, Duncan HF, Pitt Ford TR, Luder HU (2008) Histological, ultrastructural and quantitative investigations on the response of healthy human pulps to experimental capping with mineral trioxide aggregate: a randomized controlled trial. *International Endodontic Journal* **41**, 128–50.

Nekoofar MH, Adusei G, Sheykhrezae MS, Hayes SJ, Bryant ST, Dummer PM (2007) The effect of condensation pressure on selected physical properties of mineral trioxide aggregate. *International Endodontic Journal* **40**, 453–61.

Nekoofar MH, Aseeley Z, Dummer PM (2010a) The effect of various mixing techniques on the surface microhardness of mineral trioxide aggregate. *International Endodontic Journal* **43**, 312–20.

Nekoofar MH, Stone DF, Dummer PM (2010b) The effect of blood contamination on the compressive strength and surface microstructure of mineral trioxide aggregate. *International Endodontic Journal* **43**, 782–91.

Nekoofar MH, Oloomi K, Sheykhrezae MS, Tabor R, Stone DF, Dummer PM (2010c) An evaluation of the effect of blood and human serum on the surface microhardness and surface microstructure of mineral trioxide aggregate. *International Endodontic Journal* **43**, 849–58.

Nekoofar MH, Davies TE, Stone D, Basturk FB, Dummer PM (2011) Microstructure and chemical analysis of blood-contaminated mineral trioxide aggregate. *International Endodontic Journal* **44**, 1011–8.

Neville AM (2000) *Properties of concrete*, 4th edn. Essex, England: Pearson Education Limited.

Parirokh M, Asgary S, Eghbal MJ, Kakoei S, Samiee M (2011) A comparative study of using a combination of calcium chloride and mineral trioxide aggregate as the pulp-capping agent on dogs' teeth. *Journal of Endodontics* **37**, 786–8.

Saghiri MA, Asgar K, Lotfi M, Garcia-Godoy F (2012) Nanomodification of mineral trioxide aggregate for enhanced physiochemical properties. *International Endodontic Journal* **45**, 979–88.

Saliba E, Abbassi-Ghadi S, Vowles R, Camilleri J, Hooper S, Camilleri J (2009) Evaluation of the strength and radiopacity of Portland cement with varying additions of bismuth oxide. *International Endodontic Journal* **42**, 322–8.

Sestak J, Mares J, Hubik P (2010) *Amorphous and nano-crystalline materials: thermal physics, analysis, structure and properties*. Dordrecht: Springer.

Shokouhinejad N, Nekoofar MH, Razmi H *et al.* (2012) Bioactivity of EndoSequence root repair material and bioaggregate. *International Endodontic Journal* **45**, 1127–34.

da Silva GF, Guerreiro-Tanomaru JM, Sasso-Cerri E, Tanomaru-Filho M, Cerri OS (2011) Histological and histomorphometrical evaluation of furcation perforations filled with MTA, CPM and ZOE. *International Endodontic Journal* **44**, 100–10.

Torabinejad M, White D (1995) Tooth filling material and method of use. Patent 5415547 USP to Patent full Text and Image Database. Loma Linda University, USA.

Torabinejad M, Watson TF, Pitt Ford TR (1993) Sealing ability of a mineral trioxide aggregate when used as a root end filling material. *Journal of Endodontics* **19**, 591–5.

Torabinejad M, Hong CU, McDonald F, Pitt Ford TR (1995) Physical and chemical properties of a new root-end filling material. *Journal of Endodontics* **21**, 349–53.

Vivan RR, Zapata RO, Zeferino MA *et al.* (2010) Evaluation of the physical and chemical properties of two commercial and three experimental root-end filling materials. *Oral Surgery Oral Medicine Oral Pathology Oral Radiology and Endodontics* **110**, 250–6.

Zarrabi MH, Javidi M, Jafarian AH, Joushan B (2010) Histologic assessment of human pulp response to capping with mineral trioxide aggregate and a novel endodontic cement. *Journal of Endodontics* **36**, 1778–81.

Zeferino EG, Bueno CE, Oyama LM, Ribeiro DA (2010) Ex vivo assessment of genotoxicity and cytotoxicity in murine fibroblasts exposed to white MTA or white Portland cement with 15% bismuth oxide. *International Endodontic Journal* **43**, 843–8.

Zhao W, Wang J, Zhai W, Wang Z, Chang J (2005) The self-setting properties and *in vitro* bioactivity of tricalcium silicate. *Biomaterials* **26**, 6113–21.